Mechanism and Machine Theory 45 (2010) 408–425

Contents lists available at ScienceDirect

Mechanism and Machine Theory

journal homepage: www.elsevier.com/locate/mechmt

The ability of underactuated hands to grasp and hold objects ☆

Gert A. Kragten *, Just L. Herder

Delft University of Technology, Department of BioMechanical Engineering, Mekelweg 2, 2628 CD Delft, The Netherlands

ARTICLE INFO

Article history:
Received 27 July 2009
Received in revised form 28 September 2009
Accepted 9 October 2009
Available online 18 November 2009

Keywords:
Underactuation
Robotic hands
Performance
Grasping
Holding

ABSTRACT

In order to calculate *and* measure the performance of underactuated hands to pick up and move various objects, two new performance metrics have been defined. These metrics quantify the capability to achieve stable grasp equilibrium of a range of freely moving objects (*ability to grasp*), and the capability to keep hold of the grasped objects while disturbing forces are applied (*ability to hold*). The calculations and measurements of these metrics are shown for cable-pulley driven hands.

1. Introduction

Many different kinds of dexterous robotic hands have been developed for the purposes of grasping various objects (e.g. [1]). To limit their control effort, weight, and costs, specific attention has been given to the field of underactuated robotic hands. Underactuated hands have fewer actuators (DoA) than degrees of freedom (DoF). Examples of such hands and their intended application area are, for instance, the prosthetic FDD-hand [2] consisting of three actuated fingers and two passive fingers with a total of 5 DoF and 1 DoA; the five-fingered prosthetic hand developed at Keio University [3] (15 DoF, 1 DoA); the SARAH [4] intended for space applications which consists of three fingers (10 DoF, 2 DoA); and the pneumatically driven TWIX-hand [5] intended for industrial applications (6 DoF, 1 DoA). More examples of this can be found in [6]. Due to the underactuation of these hands, the fingers intrinsically conform to the shape of the objects. Such hands are therefore able to grasp a variety of objects without controlling the closing motion of the digits. This means that underactuated hands may constitute an affordable yet effective category of grippers suitable for picking up and placing operations with different objects in unstructured environments.

The ability of an underactuated hand to pick up and move different objects is mainly determined by the mechanical design of the fingers. In contrast to fully actuated hands, neither the closing motion of underactuated fingers nor the relative contact forces of the phalanges with the object – which strongly influence grasp performance – can be actively controlled. When designing well-functioning underactuated hands, performance must therefore be viewed as an important criterion at an early stage in the mechanical design process. However, grasp performance is not unambiguously defined in the literature. In addition, as is pointed out in [7,8], well-known performance metrics like form-closure and force-closure are not applicable to underactuated hands.

☆ This paper is an extension of the paper published at the IEEE International Conferences on Robotics and Automation, Kobe, Japan, May 12–17, 2009.

* Corresponding author. Tel.: +31 15 278 5633; fax: +31 15 278 4717.
E-mail addresses: g.a.kragten@tudelft.nl (G.A. Kragten), j.l.herder@tudelft.nl (J.L. Herder).

0094-114X/$ - see front matter © 2009 Elsevier Ltd. All rights reserved.
doi:10.1016/j.mechmachtheory.2009.10.002

To lend a degree of uniformity to performance metrics, the European Robotics Research Network (EURON) has taken the initiative to define benchmark tests for manipulating and grasping [9]. One of these tests involves performance in the areas of picking up and moving operations. In an effort to distinguish two phases in these operations, EURON proposed assessing the statically applied picking up forces to the grasped object in order to evaluate the picking or *grasping phase*. When it came to the *holding phase*, they proposed that the maximum permitted acceleration in different moving directions should be determined before the grasped object is lost. However, in the case of underactuated hands the skills of grasping and holding objects are still hardly ever addressed as criteria in the design stage. The same is true of the evaluation stage.

The main objective of this paper is to determine performance metrics that address the ability of underactuated hands to grasp and hold different objects. These metrics should not only facilitate the assessment of picking up and moving performance in the *evaluation* stage of realized prototypes, but they should also be especially instrumental in the analysis, understanding and optimization of such performance in an early stage of *design*. A further main objective is to assess the proposed metrics by means of simulations as well as experiments.

The paper is structured as follows: First, a literature survey is provided on the performance metrics that were used as design criteria or as evaluation criteria for underactuated hands. The new performance metrics that assess the ability to grasp and the ability to hold different objects are then defined and quantified. These new metrics are based on a combining and extending of the metrics obtained from literature and are inspired by the EURON benchmark initiatives. Section 4 introduces a general approach to calculating the new performance metrics by means of a static grasp model. The application of this model to a cable-pulley driven underactuated hand with two fingers is shown in Section 5. The calculated results of the ability to hold are also experimentally verified on a platform. The calculated and measured results are summarized in Section 6 and that is followed by the discussion and conclusions in Sections 7 and 8.

2. Grasp performance metrics in the relevant literature

Within the somewhat extensive field of grasp performance metrics, a distinction can be made between metrics that assess performance as the ability to ignore the effect of force disturbances on the grasped object on the one hand, and as the ability to cope with position disturbances on the other hand. In [10], common ways of assessing the performance of fully actuated hands are reviewed. The notions of *form-closure* and *force-closure* determine the ability to apply arbitrary external forces to the object without violating the constraints at the contact points between fingers and object. The notion of *grasp stability* is used to determine whether a grasped object returns to its reference position after (infinitesimal) disturbing displacements. The calculation of form or force-closure and grasp stability conventionally assumes that there is active control and adaptation of the individual contact forces. However, in the case of underactuated hands such active control is impossible. Instead, the fingers passively reconfigure after the grasped objects have been disturbed. For underactuated hands specific grasp performance metrics are therefore developed.

This section provides an overview of various grasp performance metrics which is based on the literature available on the design and evaluation of robotic hands with underactuated fingers (i.e. robotic hands that only reveal underactuation between the fingers are not considered). Normally a combination of different metrics is used for design optimization or evaluation. The next two subsections divide the metrics into the ones that do not require object property specification, and the metrics where the size and shape of the objects to be grasped do need to be specified. This section concludes with a number of observations.

2.1. Performance metrics that do not consider specific objects

The metrics from literature that do not consider the size, shape or position of objects can be subdivided into the metrics that assess the closing motion of the fingers and those that assess the (relative) magnitude of the contact forces. In the latter case, assumptions are made concerning the contact point positions on the phalanges.

2.1.1. Closing motion

The closing motion of underactuated fingers is related to the way in which the actuation torque is distributed over the joints by the finger mechanism and to the stiffness and preload of the joints. The following two performance metrics were found in connection with the closing motion of the fingers:

1. **Natural Closing Motion:** It is especially the underactuated fingers used in hand prostheses that are designed to resemble a natural or anthropomorphic closing motion. For instance, the design variables of the fingers of the Cyberhand [11] are optimized by matching its closing motion to known data about the natural closing motion of a human finger. What is more common is the notion that finger flexion has to start proximally and continue distally to reproduce the kinematics of the hand, as seen in the design of, for example, the RTRII [12] and the LARM-hand [13].

2. **Finger Workspace:** The driving mechanism of the fingers of the Graspar [14] is designed to maximize the workspace of the finger from a fully open to a fully flexed position without any collision with the palm. The evaluation of the achievable joint motion (as a function of the actuator force) has been published for the ultralight anthropomorphic hand [15], the Cyberhand [16], and the five-fingered prosthetic hand designed by Kamikawa and Maeno [3].

2.1.2. Contact forces

The contact forces applied to the objects by the phalanges all depend on the mechanical design and are a function of the configuration of the fingers. This configuration consists of the rotation angles of the phalanges and the location of the contact points of the object in relation to the phalanges. Since the performance metrics reviewed in this subsection consider no specific object properties, assumptions need to be made concerning the expected finger configurations. Normally, the contact points are assumed to be in the middle of all the phalanges, while the performance is assessed in a range of phalanx angles. The following four metrics were found:

1. **Positiveness:** When grasping, phalanges can generally only apply positive (i.e. compressive) contact forces to the object grasped. In configurations that require negative contact forces for the fingers to be in equilibrium, the fingers must then reconfigure. This causes loss of one or more contact points with the object. The configurations in which the underactuated fingers are in equilibrium or reconfigure to an equilibrium configuration can be described by a *Grasp Stability Plane* [6]. Maximizing the range of configurations in which the fingers can apply positive contact forces to the object is a strategy that is used in the design of, for instance, the TWIX-hand [5]. In addition, the existence of a contact point where there is a positive contact force on the distal phalanx in any configuration is sometimes used as a criterion, like in the design of the MARS and SARAH [4].
2. **Distribution:** If the ratio of the finger contact force is equal to one this is often seen as optimal due to the uniform distribution of the forces on the surface of the object. Such fingers are called force isotropic. Force-isotropy is applied as a criterion in the design of, for example, the Soft Gripper [17], and the Force-Isotropic Finger [18], where the contact points were in the middle of the phalanges. Instead of having isotropic contact forces, Fite et al. [19] aimed to achieve isotropic joint torques, while the BarrettHand [20] is able to adjust the relative joint torque by means of a torque-switch designed to get feedforward control over the distribution of the contact forces.
3. **Magnitude:** There are different possible criteria regarding the magnitude of the contact forces. Minimum contact force at the tip of the fingers was required when designing the SPRING-hand [21] and when evaluating the prototype of the KNU-hand [22]. Maximizing the contact forces relative to the actuation force was what was required with the TH-1, the TH-2 [23,24], and for the RL1 [25]. In order to achieve intuitive force feedback a constant magnitude of the contact forces relative to the actuation torque and independent of the configuration of the finger was implemented as a performance metric in the design and evaluation of the FDD-hand [2]. In the design of the Subcentimetre Grasper [26], minimum contact forces were required at the proximal phalanx while the distal phalanx was still not in contact with the object.
4. **Resultant Force Direction:** One may consider the resultant of the contact forces of all the phalanges of one finger. Its working direction has to be towards the palm of the hand and towards the fingers attached to the opposite side of the palm. It is therefore likely that the force disturbances on a grasped object that radiate from the hand will be counteracted by the resulting contact force. This was a criterion applied by Boudreault and Gosselin [26].

2.2. Performance metrics when considering specific objects

This section provides an overview and a classification of the performance metrics of underactuated fingers in relation to contact with specific objects. In contrast to the criteria given in the previous section, assumptions need to be made concerning the shape, size and position of the object. In addition to assessing the performance by means of the characteristics of the contact forces on objects, various metrics were established on the successful grasping of objects and on the ability to hold grasped objects with the hands.

2.2.1. Contact forces on grasped objects

The criteria for the contact forces on grasped objects are essentially the same as the criteria applied when specific objects are not considered. However, in this particular case the position of the contact points and the rotation angles of the phalanges required to achieve the contact forces are not based on assumptions but are instead derived from the configurations where grasp equilibrium is achieved with physical objects.

1. **Distribution:** Uniform or isotropic contact force distribution along the phalanges while grasping circular objects of different sizes was used as a design criterion with, for instance, the 15 DoF anthropomorphic hand devised by Gosselin et al. [27] and evaluated by means of experiments conducted with the Soft Gripper [17] and simulations done

for the LARM-hand [13]. Instead of using force-isotropy, Kamikawa and Maeno [3] aimed to achieve a contact force ratio that was comparable to human fingers. That was their criterion when designing and evaluating their five-fingered prosthetic hand.

2. **Magnitude:** The criterion used by Gosselin et al. [27] was that of maximizing the contact forces of one finger on an object relative to the actuation torque. By contrast, when designing and evaluating the SDM-hand [28] the contact forces of all the fingers was minimized in order to avoid damaging the object grasped. The total magnitude of the contact forces on the objects grasped relative to the actuation torque is also evaluated by means of experimentation or simulation in the case of many other prototypes like the SPRING-hand [21], and the MARS and SARAH [29].
3. **Resultant Direction:** In [30,6], the criterion required to obtain a resultant contact force directed towards the palm of the hand and towards the fingers on the opposite side of the palm was developed and applied to the design of the MARS and SARAH-hands [4] and the 15 DoF anthropomorphic hand created by Gosselin et al. [27].

2.2.2. Grasping objects

Criteria on the ability to successfully grasp objects differ depending on the definition of what constitutes a successful grasp and the quantification of the range or diversity of the graspable objects. We categorize these criteria according to the definitions of what amounts to a successful grasp and indicate, per criteria, how the diversity of objects is quantified.

1. **Enveloping Objects:** If one considers a successful grasp to be the ability to envelope an object then the criterion maximizing the range of objects that can be enveloped by the fingers is used. For a set of 20 circular, rectangular and oval objects, the optimal number and relative length of the phalanges of the fingers was calculated and consequently introduced to the design of the two-fingered underactuated hand produced by Schuurmans et al. [31]. When designing the SDM-hand [28], the range of initial positions and the radii of the circular objects that could be enveloped was maximized.
2. **Equilibrium of Fingers:** Maximizing the range of objects and the object positions where the underactuated fingers could attain equilibrium while the objects (spheres, cylinders, frustums and cubes) were fixed to the environment was the design and evaluation criterion used with, for instance, the MARS and SARAH-hands [4,32].
3. **Equilibrium between Fingers and Objects:** When the object is not supported by the environment, a grasp is successful if the fingers, as well as the grasped object, are in equilibrium. To evaluate the prototypes, pictures were often just shown of successfully grasped objects from daily life situations in which different grasp taxonomies were employed, e.g. [16,33,3].

2.2.3. Holding objects

When a grasped object is manipulated or moved, the object in question must be held within the hand. The criteria applied to the holding of objects comprise both the form-closure modified for underactuated hands, and the ability to resist force and moment disturbances.

1. **Modified Form-Closure:** For non-backdriveable underactuated fingers only, the conventional way of determining form-closure was adapted to determine the minimum number of non-backdriveable elements required to obtain form-closed grasps [7]. The criterion required to achieve form-closure was applied in the design of the TWIX-hand [5].
2. **Force Disturbances:** As a performance metric, the maximum permitted external force and moments on grasped objects was experimentally evaluated for the prototypes created by Schuurmans et al. [31] and Kamikawa and Maeno [3].

2.3. Summary and observations

The different standards used in the design or evaluation phase to assess the performance of robotic hands with underactuated fingers are shown in Table 1. When we review these literature results, we observe that in the various cases considered the design and evaluation of underactuated hands has been based on a wide variety of performance metrics. However, not all of them are well quantified. The performance criteria most often used for the design of underactuated hands fail to take objects into consideration. Surprisingly, the performance metrics used in the design stage are not often used to evaluate the prototypes, if they are evaluated at all. Furthermore, the experiments carried out to evaluate the performance are rarely clearly described. It is therefore virtually impossible to compare the performance of underactuated hands on the basis of results presented in the relevant literature.

To assess the performance of underactuated hands for pick and place operations of various objects, the metrics concerning the equilibrium of the fingers and objects with respect to the grasping of the objects (2.2.3 in Table 1) and the permitted force disturbances with respect to the holding of objects (2.3.2 in Table 1) are most closely related. However, a benchmark test to calculate this performance in the design stage as well as to measure this performance in the evaluation stage still does not exist. Therefore, inspired by the performance metrics from the literature, a first step towards the definition and quantification of such benchmark test for underactuated hands is taken in the next chapter.

Table 1
Overview of the performance metrics in relation to the realizations of underactuated hands and fingers. In the table cells, the metrics applied at either the design stage or the evaluation stage of these hands, as reported in the literature, are shown as *d* and *e*, respectively. (See above-mentioned references for further information.)

	1. Metrics when not considering specific objects						2. Metrics when considering specific objects							
	1.1.1 Natural Closing Motion	1.1.2 Finger Workspace	1.2.1 Positiveness	1.2.2 Distribution	1.2.3 Magnitude	1.2.4 Resultant Direction	2.1.1 Distribution	2.1.2 Magnitude	2.1.3 Resultant Direction	2.2.1 Enveloping Objects	2.2.2 Equilibrium Fingers	2.2.3 Equilibrium between Fingers and Objects	2.3.1 Modified Form-Closure	2.3.2 Force Disturbances
BarrettHand [20]	d			d										
Ca.U.M.Ha. [34]	d											e		
Cyberhand [16,35,11]	d,e	e		d								e		
6 DoF Delft hand [31]				d						d		e		e
FDD-hand [36,2]			d	d,e	d,e									
Force-Isotropic Finger [18,37]			e	d										
Gas-actuated hand [19]				d								e		
Gloveless prosthetic hand [38]	d				e			e				e		
Graspar [14]	d	d										e		e
HIT/DLR hand [39]	e				e							e		
15 DoF Keio hand [3]		e					d,e					e		e
KNU-hand [22]					e							e		
LARM-hand [13]	d			d			e	e						
15 DoF Laval hand [27]							d	d,e	d		d	e		
MARS, SARAH [4,29,32]			d				d	d,e	d		d,e	e		
Optimal Laval fingers [40]			d	d										
RL1 [25]					d							e		
RTR-2 [41,12]	d		d					e						
Soft Hand [42]								e				e		
Soft Gripper [17]				d			e				e			
SDM-hand [28,33]								d,e		d,e		e		
Southampton WAM [43,44]	d													
SPRING-hand [21]	d				d			e						
Subcentimetre Gripper [26]	d,e			d,e	d	d								
TH-1, TH-2 [23,24]	d				d							e		
TUAT/Karlsruhe hand [45]	d											e		
TWIX-hand [5]			d	d								e	d	
Ultralight hand [15]		e			e							e		

3. Define and quantify the ability to grasp and hold

In 'pick and place' operations, the object first has to be *grasped* by the hand. This means that the fingers have to exert compressive contact forces on the object, while the equilibrium and stability conditions of the fingers and the object are satisfied. The object must then be *held* in the hand while it is subjected to disturbances like acceleration created by a robotic arm. These disturbances can be viewed as external forces applied to the object, which must be resisted by the contact forces of the fingers in order to maintain grasp equilibrium (although not necessarily required in the initial configuration). We therefore qualitatively define the ability to grasp and hold as follows:

- "The *ability to grasp* means being able to achieve stable equilibrium in a range of freely moving objects just using the fingers (and palm) of the hand."
- "The *ability to hold* means being able to keep the grasped objects in the hand while disturbing forces are applied on the objects."

To quantify these performance metrics by means of a dimensionless scalar, the properties of the objects and external disturbing forces must be standardized. We initially propose considering rigid, lightweight, cylindrical objects grasped around the curved surface. Cylindrical objects have a continuous surface, are orientation independent around their principal axis, and have a size that can be described using one variable (i.e. the radius r_{obj}). By limiting ourselves to cylindrical objects, the calculation and experimental testing of the performance linked to the grasping and holding of objects is simplified. Besides, in the domestic environment most objects tend to be approximately cylindrically shaped, like for instance door handles, hand supports, cups and bottles [46]. The range of graspable objects can be expressed by calculating the difference between the radius of the largest and the smallest cylinder Δr_{obj} for which stable grasp equilibrium exists. To normalize this value, it was established that in the case of grasps where there was no friction between the fingers and the object, at least half of the circumference of the object should be enveloped by the fingers and the palm to achieve equilibrium. Therefore, we propose quantifying the *ability to grasp* as follows:

$$Q_{grasp} = \frac{\pi \Delta r_{obj}}{S_{hand}} \tag{1}$$

where S_{hand} is the span of the hand, i.e. the total length of two opposing fingers and the width of the palm. With frictionless grasping a performance of at most 100% can thus be attained. Only for grasps where there is friction can the performance be greater. The quantification of this metric matches the intuitive evaluation of robotic hands as shown in various studies where pictures are given of objects of different sizes being grasped (e.g. [16]).

The disturbing forces on the grasped objects are initially regarded as forces of constant magnitude applied to the center of mass of a stably grasped object. The maximum permitted disturbing force F_h is regarded as the force at which the object of known radius r_{obj} can still be held inside the hand, irrespective of the working direction Ψ of this force. Note that the critical working direction in which the object is most easily pulled out by the disturbing forces is not a priori known which is why different working directions must be investigated. To normalize F_h, it is considered that the contact forces of underactuated fingers – and hence F_h – are linearly related to the magnitude of the actuation torque T_a of the fingers. Therefore, we propose quantifying the *ability to hold* as follows:

$$Q_{hold} = \min_{\Psi} \frac{F_h}{T_a/L} \tag{2}$$

where $\min_{\Psi} F_h$ is the minimum of the maximum permitted disturbing forces of all the investigated working directions, where T_a/L is the actuation torque of the fingers with respect to the object initially grasped divided by the length of the fingers in order to make Q_{hold} dimensionless. The quantification of this metric corresponds to the evaluation of robotic hands given in the literature and obtained by measuring the pulling force required in various directions to pull out objects (e.g. [3]). In addition, if we consider the notion of d'Alembert forces, this metric closely relates to the benchmark test proposed by EURON for the holding phase [9], which involves considering the maximum permitted acceleration in different moving directions before the grasped object is lost.

4. Grasp model

To calculate or predict the ability to grasp and hold cylindrical objects in underactuated hands at an early design stage, a simple static model was developed. This model takes into account the fact that underactuated fingers passively reconfigure when grasping objects, but also when external forces are applied to the grasped object. Note that this model is applicable to any conventional underactuated hand, such as hands with fingers that are driven by a cable, cable-pulley, linkage, or differential gear mechanism. In this paper, we ignore friction and gravity, we assume that there are rigid contact points between the objects and the fingers, and we consider objects that are able to move in a plane. The underactuated hand in this model consists of two identical fingers with a distance of $2B$ between the proximal joints and a straightened palm width of t_p in between, as shown in Fig. 1. Each finger consists of N straight phalanges l_{ij} long and t_{ij} width between the contact surface

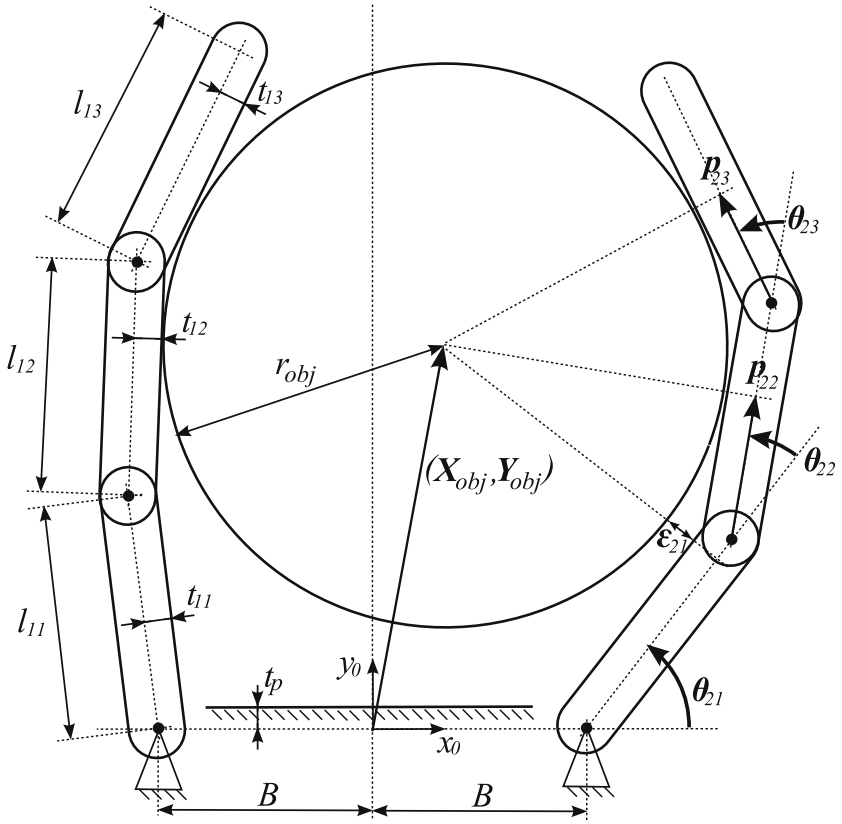

Fig. 1. Schematic drawing of a planar hand, consisting of two fingers each with three phalanges grasping a circular object with a radius of r_{obj} and in position (X_{obj}, Y_{obj}) with respect to the global frame (x_0, y_0). For the sake of clarity, the dimensions are only given on the left finger, while the finger configuration variables are only given on the right finger. The phalanges have a length of l_{ij} and a width of t_{ij} between the center line and contact area, where $i = 1, 2$ denotes the left and right fingers, respectively, and $j = 1, 2, \ldots N$ denotes the proximal, second and distal phalanxes, respectively. θ_{ij} and p_{ij} are the relative phalanx rotations and contact positions, while ϵ_{ij} is the gap between the ijth phalanx and the object. The distance between the proximal joints of the fingers is $2B$, while the flat palm in between has a width of t_p.

and the center line. i $(i = 1, 2)$ represents the finger number with 1 as the left finger and 2 as the right finger; j $(j = 1, 2, \ldots, N)$ indicates the phalanx number, in which 1 is the proximal phalanx, and N is the distal phalanx. The static grasp model calculates the feasible grasp configurations of the fingers as a function of the object position, comprising the phalanx angles θ_{ij} and contact point positions p_{ij}.

4.1. Calculating finger configurations

To determine a feasible configuration for the fingers while grasping an object, a set of nonlinear geometric and force equalities or constraints for each phalanx must be iteratively solved. The contact between phalanx ij and the object can be geometrically described according to the following loop closure vector equations:

$$\mathbf{A}\left(\begin{pmatrix} B \\ 0 \end{pmatrix} + \sum_{k=1}^{j-1} \prod_{m=1}^{k} \mathbf{R}_{\theta_{im}} \begin{pmatrix} l_{ij} \\ 0 \end{pmatrix} + \prod_{m=1}^{j} \mathbf{R}_{\theta_{im}} \begin{pmatrix} p_{ij} \\ t_{ij} + \epsilon_{ij} \end{pmatrix}\right) = \begin{pmatrix} X_{obj} \\ Y_{obj} \end{pmatrix} + \mathbf{A} \prod_{m=1}^{j} \mathbf{R}_{\theta_{im}} \begin{pmatrix} 0 \\ -r_{obj} \end{pmatrix} \tag{3}$$

where the left-hand side and right-hand side of the equation account for the contact point on the phalanges and the object. The symbols and sign convention are further explained by Fig. 1. X_{obj} and Y_{obj} are the position of the cylindrical object with radius r_{obj}, and $\mathbf{A}$ and $\mathbf{R}_{\theta_{ij}}$ represent the following respective rotation matrices:

$$\mathbf{A} = \begin{bmatrix} -1^i & 0 \\ 0 & 1 \end{bmatrix} \tag{4}$$

$$\mathbf{R}_{\theta_{ij}} = \begin{bmatrix} \cos(\theta_{ij}) & -\sin(\theta_{ij}) \\ \sin(\theta_{ij}) & \cos(\theta_{ij}) \end{bmatrix} \tag{5}$$

The magnitude of the contact force normally applied to the object surface by the phalanx ij of an underactuated finger was been derived by Birglen et al. [6]. With underactuated fingers, the relative magnitude of the contact forces of the phalanges when the finger is at rest depends on the configuration of the finger. If one adapts the notation of Birglen et al. [6], and ignores the return springs or mechanical stops, these contact force equations are as follows:

$$F_{ph_{ij}} = \frac{R_{ij}}{p_{ij}} T_a - \sum_{k=j+1}^{N} \left(\sum_{m=j}^{k-1} l_{im} \cos \left(\sum_{n=m+1}^{k} \theta_{in} \right) + p_{ik} \right) \frac{F_{ph_{ik}}}{p_{ij}} \tag{6}$$

where T_a is the input actuation torque of the finger, and R_{ij} is the transmission ratio or distribution of the actuation torque to the ijth phalanx ($R_{i1} = 1$). This transmission ratio R_{ij} can be a function of the grasp configuration as well, depending on the type of underactuated finger mechanism. In the next chapter, Eqs. (3) and (6) will be elaborated in connection with a particular example of a cable-pulley driven underactuated finger.

In the case of a feasible grasp configuration, phalanges that are in contact with the object satisfy Eq. (3) where the space ϵ_{ij} between these phalanges and the object surface is zero. In addition, the contact forces evaluated by Eq. (6) are positive (i.e. compressive contact forces), and the calculated contact point positions p_{ij} lie on the physical part of the phalanges:

$$F_{ph_{ij}} > 0 \tag{7}$$

$$0 < p_{ij} < l_{ij} \tag{8}$$

Regarding phalanges that are not in contact with the object, their contact force equation (6) equals zero, and the space ϵ_{ij} is positive:

$$F_{ph_{ij}} = 0 \tag{9}$$

$$\epsilon_{ij} > 0 \tag{10}$$

where ϵ_{ij} is obtained by rearranging Eq. (3).

In the iterative calculation done to obtain a feasible finger configuration for an object with a known radius and position, a solution is first calculated for a situation in which all the phalanges are in contact based on Eq. (3). The calculated phalanx angles and contact positions are then substituted in Eq. (6) and validated with respect to their feasibility according to Eqs. (7) and (8). If some phalanges do not satisfy the constraints (i.e. because the contact force is negative or the contact is not on the physical part of the phalanx), a new configuration has to be calculated based on Eq. (9) for those phalanges, while Eq. (3) still applies to the phalanges which had a feasible contact point with the object. This procedure continues until a good solution is found. If no feasible solution can be found at all, no equilibrium of the fingers on the object with that particular radius r_{obj} and position (X_{obj}, Y_{obj}) can be said to exist.

When a feasible configuration of the fingers on the surface of the object at (X_{obj}, Y_{obj}) is calculated, the effect of the contact forces $\vec{F}_c$ on the grasped object (expressed in terms of the global coordinate frame) can be calculated as follows:

$$\vec{F}_c = \sum_{i=1}^{2} \left(\mathbf{A} \sum_{j=1}^{N} \prod_{k=1}^{j} \mathbf{R}_{\theta_{ik}} \begin{pmatrix} 0 \\ F_{ph_{ij}} \end{pmatrix} \right) \tag{11}$$

This way of calculating a feasible finger configuration and the contact forces by means of Eqs. (3)–(11) for a particular object position can be extended to numerically calculating the effect of the contact forces on an object as a function of the object position. A contact force vector field is thus obtained, which will form the basis for calculating the performance in terms of the ability to grasp and hold. In addition, the work W required to move the object can be calculated, which allows us to determine, for instance, the stability of the grasp equilibrium points. Since we have ignored friction, we can calculate $\Delta W_{A,B}$ to move from $(X_{obj}, Y_{obj})_A$ to $(X_{obj}, Y_{obj})_B$ by taking the opposite of the work delivered by the actuator. If we assume that the actuation torque is constant, and if we calculate the corresponding actuator displacement according to the relative phalanx angles times the transmission ratios, then the relative work will be as follows:

$$\Delta W_{A,B} = -T_a \sum_{i=1}^{2} \sum_{j=1}^{N} \left(R_{ij_B} \theta_{ij_B} - R_{ij_A} \theta_{ij_A} \right) \tag{12}$$

where θ_{ij_A} and θ_{ij_B}, and R_{ij_A} and R_{ij_B} are the phalanx angles and the transmission ratios belonging to the finger configuration at object position $(X_{obj}, Y_{obj})_A$ and $(X_{obj}, Y_{obj})_B$, respectively. When ΔW is positive that means that moving the object from A to B requires work.

4.2. Calculating the ability to grasp

The *ability to grasp* is defined as the capability to achieve stable equilibrium in a range of freely moving objects with the fingers and palm of the hand. Grasp equilibrium means that with a feasible finger configuration the resultant of the contact forces on the object is zero:

$$\vec{F}_c = \begin{pmatrix} 0 \\ 0 \end{pmatrix} \tag{13}$$

Stability means that the object and the fingers have an energy minimum. For conservative systems, the grasp is stable if the real parts of the eigenvalues of the stiffness matrix $\mathbf{K}$ are negative, where $\mathbf{K}$ is obtained from numerical differentiation of the resultant contact force in the equilibrium configuration.

To calculate the stable grasp equilibrium positions of a cylindrical object with a known radius r_{obj}, the loop closure vector equations (Eq. (3)) and the object equilibrium condition (Eq. (13)) first have to be iteratively solved to obtain the unknown finger configurations $\theta_{ij},\ p_{ij}$, and the object position (X_{obj}, Y_{obj}). The calculated phalanx angles and contact positions are then substituted in the contact force equations (Eq. (6)) and the feasibility is verified by Eqs. (7) and (8). In addition one has to verify whether, for the equilibrium configuration obtained the object or finger tips collided with the palm:

$$Y_{obj} > r_{obj} + t_p \tag{14}$$

$$\sum_{m=1}^{N} l_{im} \sin\left(\sum_{n=1}^{m} \theta_{in}\right) > 0 \tag{15}$$

where t_p is the width of the palm as is shown in Fig. 1. Finally, the stability of the equilibrium configuration is verified. If for some phalanges Eq. (7) or (8) is violated, a new equilibrium configuration is calculated in the way described in the previous section. If Eq. (14) is violated, a new configuration is calculated in which the object touches the palm while the result of the contact forces of the phalanges indicates that the object is pushing against the palm:

$$Y_{obj} = r_{obj} + t_p \tag{16}$$

$$\vec{e}_Y^T \vec{F}_c < 0 \tag{17}$$

where $\vec{e}_Y^T$ denotes the transposed unity vector in the Y-direction. If no feasible solution can be calculated at all then it is assumed that the object is too large or too small to be stably grasped.

To calculate the radius of the smallest and the largest cylinders that can be stably grasped, we propose using a grid search because of the strong nonlinearity of the equations and the constraints. By gradually decreasing or increasing the radius of the object until no stable grasp equilibrium position can be calculated, the smallest and largest radii can be obtained. Finally, Q_{grasp} can be calculated according to Eq. (1).

4.3. Calculating the ability to hold

The *ability to hold* is defined as the ability to keep the grasped objects inside the hand while disturbing forces are applied to the objects. To adapt the contact forces so that they can resist these disturbing forces, underactuated fingers – except for the non-backdriveable ones – have to passively reconfigure while the object undergoes a finite displacement. To calculate the maximum permitted force disturbance in direction Ψ relative to the palm, we introduced a gradual displacement of the object in this direction (i.e. parallel to vector u), while the object was free to move in the perpendicular direction v, see Fig. 2. The fingers therefore had to adapt to a new grasp configuration in which the effect of the contact forces on the object F_c was parallel to the working direction of the disturbing force, while F_c was zero in the freely moving direction of the object:

$$(\mathbf{R}_\Psi \vec{e}_v)^T \vec{F}_c = 0 \tag{18}$$

where $\vec{e}_v$ was the unity vector in the direction of v, and $\mathbf{R}_\Psi$ was the rotation matrix similar to Eq. (5). By calculating the magnitude of F_c and the new equilibrium position of the object perpendicular to the imposed displacement in accordance with similar equations to those given in the previous sections, a force–displacement characteristic could be obtained. The maximum of this characteristic, which was oppositely directed with respect to the disturbance direction, is seen as the maximum permitted disturbing force F_h in that particular direction:

$$F_h = \max_u \left(-(\mathbf{R}_\Psi \vec{e}_u)^T \vec{F}_{c,u}\right) \tag{19}$$

where u is the object displacement parallel to the working direction of the disturbing force.

The force required to pull an object out of the hand, starting from a stable grasp equilibrium configuration, depends on the pulling direction u. However, the direction in which the required force is at its minimum is not a priori known. In fact, it was expected that this direction would depend on the mechanical design choices. We thus initially proposed applying external forces in distinct directions and determining the direction in which the required force is at its minimum.

5. Application to a cable-pulley driven hand

In order to demonstrate the procedure and its usefulness, the newly developed metrics that quantify the ability to grasp and hold were then applied to the evaluation of the performance of a cable-pulley driven, planar, underactuated hand. This hand consists of two identical fingers and a palm like the schematic hand shown in Fig. 1. The driving mechanism of the fingers consists of one cable wrapped around pulleys like the fingers of the Soft Gripper [17]. Each pulley can freely rotate, except for the distal pulley which is connected to the distal phalanx. To demonstrate the effect that the number of phalanges has on the performance, we modeled a hand consisting of fingers with two phalanges as well as a hand with three-phalanx fingers. The expected performance was calculated for both hands. In the case of the hand consisting of fingers with two phalanges, the ability to hold was verified by experiments.

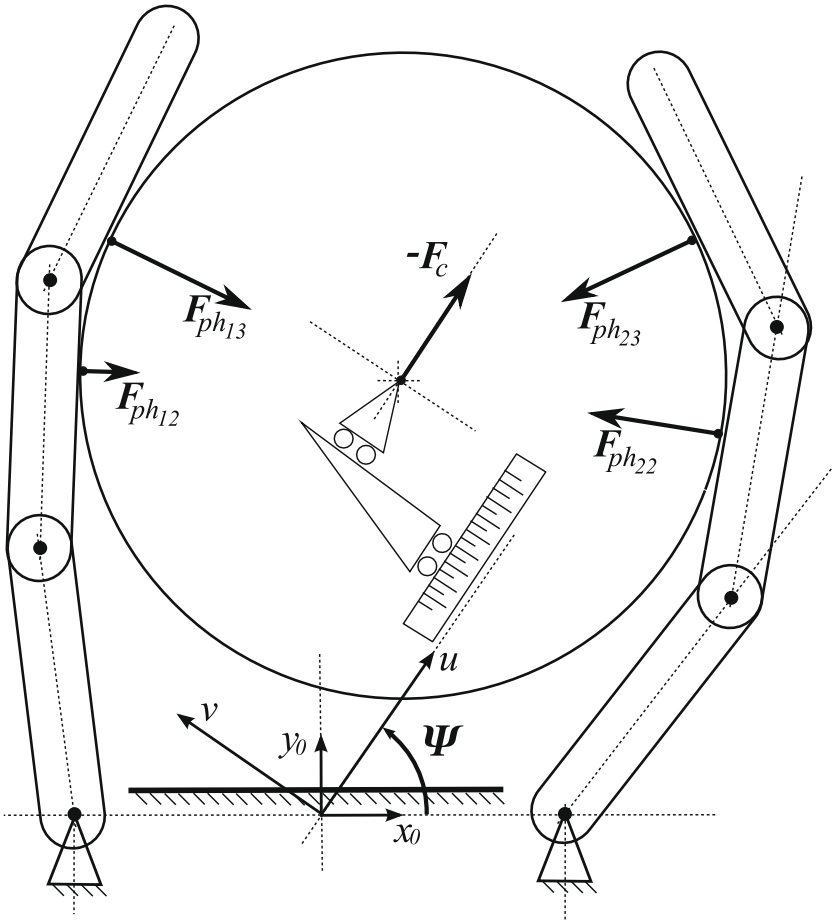

Fig. 2. Schematic view of the disturbance model in which a grasped object is gradually displaced in the u direction, while being free to move in the perpendicular direction v. Frame (u, v) is rotated at angle Ψ relative to the global frame (x_0, y_0). In each displacement step, the fingers passively reconfigure and the external force required to keep the object in the new position $u + \Delta u$ is calculated as the result of the contact forces $F_{ph_{ij}}$ in the opposite direction.

5.1. Performance calculation

Schematic representations of the fingers of the underactuated hands with all the relevant symbols are shown in Fig. 3. The fingers of both hands each have the same total length L, which is equally divided over the phalanges. All the fingers are actuated by the same constant actuation force. The transmission ratios – which in this case are equal to the ratio of the radii of the pulleys with respect to the radius of the proximal pulley r_1 – were chosen as follows:

$$R_{ij} = \frac{r_j}{r_1} = \sum_{n=j}^{N} \frac{l_n}{L} \tag{20}$$

where N is the number of phalanges per finger, and l_n is the length of the nth phalanx. The dimensions of the fingers are given in Table 2, which followed from the approximately 2:1 scaling of the length of a human finger.

For both hands the loop closure vector equations (Eq. (3)) and the contact force equations (Eq. (6)) are elaborated. For reasons of space, only the elaboration of these equations for the right finger with three phalanges is provided here, while the elaboration for the right finger with two phalanges can be found in [47]:

$$\begin{pmatrix} B \\ 0 \end{pmatrix} + \mathbf{R}_{\theta_{21}} \begin{pmatrix} p_{21} \\ t + \epsilon_{21} \end{pmatrix} = \begin{pmatrix} X_{obj} \\ Y_{obj} \end{pmatrix} + \mathbf{R}_{\theta_{21}} \begin{pmatrix} 0 \\ -r_{obj} \end{pmatrix} \tag{21}$$

$$\begin{pmatrix} B \\ 0 \end{pmatrix} + \mathbf{R}_{\theta_{21}} \begin{pmatrix} l_1 \\ 0 \end{pmatrix} + \mathbf{R}_{\theta_{21}} \mathbf{R}_{\theta_{22}} \begin{pmatrix} p_{22} \\ t + \epsilon_{22} \end{pmatrix} = \begin{pmatrix} X_{obj} \\ Y_{obj} \end{pmatrix} + \mathbf{R}_{\theta_{21}} \mathbf{R}_{\theta_{22}} \begin{pmatrix} 0 \\ -r_{obj} \end{pmatrix} \tag{22}$$

$$\begin{pmatrix} B \\ 0 \end{pmatrix} + \mathbf{R}_{\theta_{21}} \begin{pmatrix} l_1 \\ 0 \end{pmatrix} + \mathbf{R}_{\theta_{21}} \mathbf{R}_{\theta_{22}} \begin{pmatrix} l_2 \\ 0 \end{pmatrix} + \mathbf{R}_{\theta_{21}} \mathbf{R}_{\theta_{22}} \mathbf{R}_{\theta_{23}} \begin{pmatrix} p_{23} \\ t + \epsilon_{23} \end{pmatrix} = \begin{pmatrix} X_{obj} \\ Y_{obj} \end{pmatrix} + \mathbf{R}_{\theta_{21}} \mathbf{R}_{\theta_{22}} \mathbf{R}_{\theta_{23}} \begin{pmatrix} 0 \\ -r_{obj} \end{pmatrix} \tag{23}$$

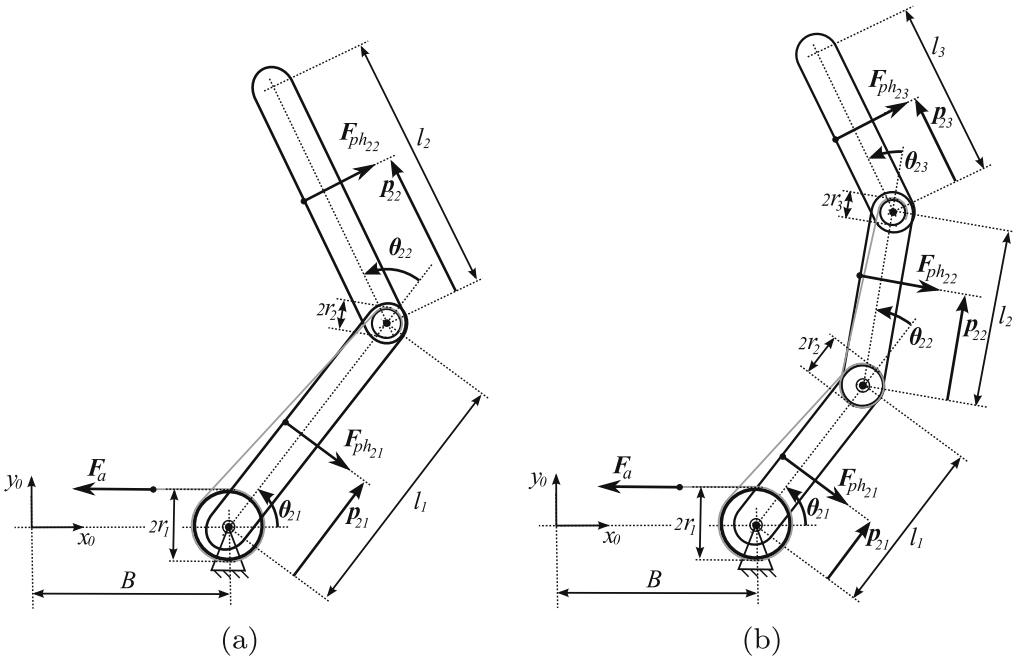

Fig. 3. Schematic illustration of the right finger consisting of two phalanges (a) and three phalanges (b), respectively. Both types of fingers are driven by one cable which is subsequently wrapped around freely rotating pulley(s) and attached to the distal pulley which is fixed to the distal phalanx. The radii of the pulleys r_j, the length l_j of the phalanges, and the magnitude of the constant actuation force F_a are given in Table 2.

Table 2
Dimensions of the underactuated fingers.

Symbol	Value	Explanation
General dimensions		
F_a	22	Actuation force in cable (N)
r_1	10.0	Radius proximal pulley (mm)
L	160	Total length of the fingers (mm)
t	8.5	Thickness of palm and phalanges (mm)
B	30.0	Half of palm width (mm)
Dimensions of two-phalanx finger		
r_2	5.0	Radius distal pulley (mm)
$l_1 = l_2$	80.0	Length proximal phalanx (mm)
Dimensions of three-phalanx finger		
r_2	6.7	Radius distal pulley (mm)
r_3	3.3	Radius distal pulley (mm)
$l_1 = l_2 = l_3$	53.3	Length proximal phalanx (mm)

$$F_{ph_{21}} = \frac{1}{p_{21}} r_1 F_a - \frac{(l_1 \cos\theta_{22} + p_{22})}{p_{21}} F_{ph_{22}} - \frac{(l_1 \cos(\theta_{22} + \theta_{23}) + l_2 \cos\theta_{23} + p_{23})}{p_{21}} F_{ph_{23}} \tag{24}$$

$$F_{ph_{22}} = \frac{r_2}{r_1 p_{22}} r_1 F_a - \frac{(l_2 \cos\theta_{23} + p_{23})}{p_{22}} F_{ph_{23}} \tag{25}$$

$$F_{ph_{23}} = \frac{r_3}{r_1 p_{23}} r_1 F_a \tag{26}$$

For both hands the work required to displace an object with a radius of $r_{obj} = 65$ mm and the contact forces on the object are calculated using `fsolve.m` in *Matlab* (version 7.5.0, The Mathworks, Natick, MA) to solve Eqs. (3)–(12) according to the method described in Chapter 4.

To determine the ability to grasp, the smallest and largest graspable object radii for both hands were calculated. Taking a cylinder with $r_{obj} = 65$ mm as the initial size, the size was gradually decreased and increased by, in each case, steps of 1 mm. For every step, a grasp equilibrium configuration was calculated using `fsolve.m` in *Matlab* to solve Eqs. (3)–(10) and (13), the feasibility and stability of the solution was also verified. The radius of the smallest and largest cylinder for which a stable grasp equilibrium exists was recorded and normalized according to the span of the hand (i.e $2L + 2B = 380$ mm).

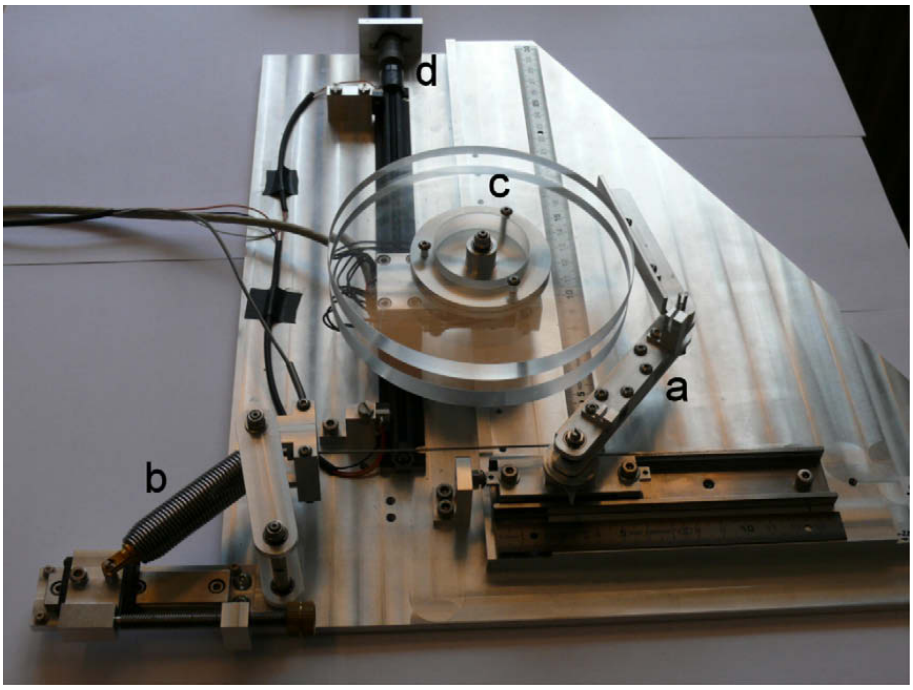

Fig. 4. Test set up with underactuated finger (a), constant force actuator (b), cylindrical object (c) and linear motor (d) in order to pull the object out of the hand at a constant velocity.

To determine the ability to hold, a cylinder of $r_{obj} = 65$ mm was displaced in 1 mm steps in the direction of $\pi/6$, $\pi/3$, and $\pi/2$ with respect to the palm starting from a stable grasp equilibrium configuration. The displacement of the object in the perpendicular direction and the resultant contact force in the direction of the imposed displacement were calculated by solving Eqs. (3)–(10) and (18) with `fsolve.m` in *Matlab*. The maximum values of the force–displacement characteristics obtained in these three directions were calculated, and the smallest maximum was taken as the ability to hold performance.

5.2. Experimental verification

Pulling cylindrical objects out of the fingers with two phalanges has been experimentally assessed on a platform as described and evaluated in [48]. On this platform we only considered disturbances along the line of symmetry (i.e. a displacement direction of $\pi/2$ with respect to the palm). A hand consisting of only one finger was thus sufficient when the object was supported by a linear actuator. The underactuated finger, as shown in Fig. 4, was made of aluminum according to the dimensions given in Table 2. The constant force actuation was mechanically obtained by attaching the cable to a spring-loaded constant force generator mechanism. It was measured with the help of a force sensor (Futek, LTH300).

To represent frictionless grasps, we created a cylindrical object consisting of two acrylic discs with a radius of 65 mm that could rotate independently around a vertical axis. In this way, instead of slipping along the phalanges, the discs roll over their contact surfaces. This is kinematically and kinetically equivalent to frictionless slipping along the phalanges. In this way we were thus able to physically emulate frictionless grasping. This object is supported and displaced by a linear actuator and moved out of the hand with a constant velocity of 1.76 mm/s.

The resultant of the contact forces F_c on the object in the direction of the displacement was measured by means of a load cell mounted between the object and the linear motor. This load cell consisted of two parallel plates of spring steel that was only compliant in the direction of displacement. With four strain gauges (HBM, 1-LY41-3/350) glued to the parallel plates and electrically connected in a Wheatstone's bridge configuration, F_c could be measured with an accuracy of 0.2 N at its full range. The output voltages of the force sensor and load cells were collected at a sample rate of about 100 Hz with an USB-DAQ (National Instruments, USB-6009) and using LabView 8.2.

6. Results

Table 3 shows the calculated performance metrics of the considered underactuated hands with two- and three-phalanx fingers, respectively. In Fig. 5 the calculated force–displacement characteristics for the object with a radius of $r_{obj} = 65$ mm are shown. The end point of these curves is determined according to the contact point reaching the tip of one of the distal phalanges. In this graph a negative force means that the fingers push the object out of the hand instead of pulling it towards the palm of the hand. The measured and calculated force–displacement characteristics in the $\pi/2$ direction with respect to the palm of the hand with fingers that consists of two phalanges are shown in Fig. 6.

Table 3
Calculated performance metrics concerning the ability to grasp (Q_{grasp}) and the ability to hold (Q_{hold}). In addition, the radius of the smallest ($\min r_{obj}$) and largest ($\max r_{obj}$) graspable object, as well as the minimum force F_h needed to displace the object completely from the hand in three directions are shown.

Performance	Two-phalanx fingers	Three-phalanx fingers
Q_{grasp} (%)	60	62
$\min r_{obj}$ (mm)	12	18
$\max r_{obj}$ (mm)	85	93
Q_{hold} (−)	0.77	0.98
$F_h(\pi/6)$ (N)	1.05	1.34
$F_h(\pi/3)$ (N)	1.25	1.58
$F_h(\pi/2)$ (N)	1.57	1.61

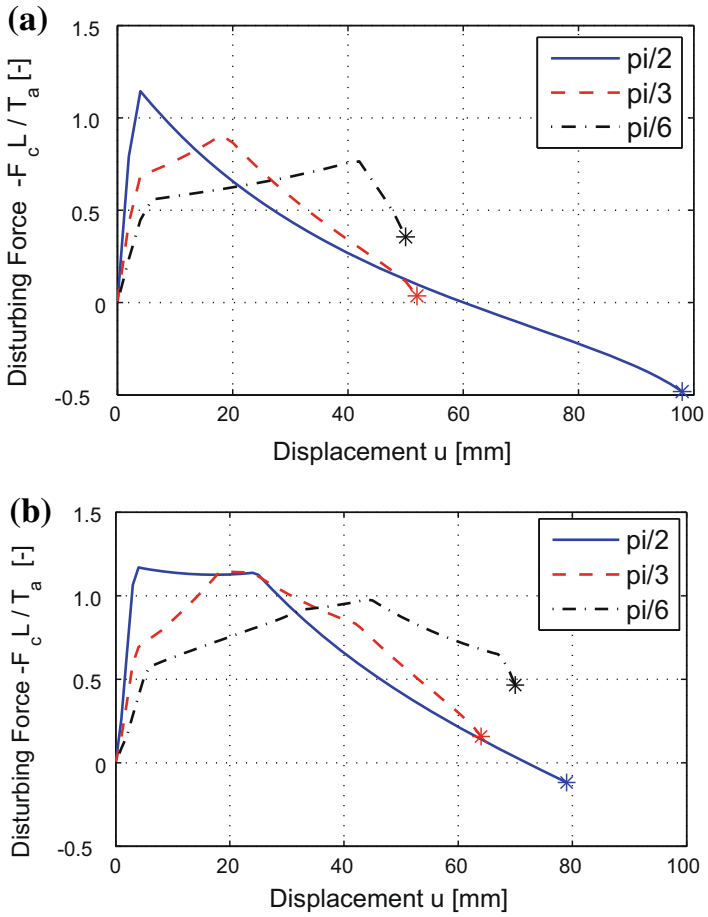

Fig. 5. Required force (normalized by the constant actuation torque T_a and finger length L) versus the displacement u in (mm) (starting from a stable equilibrium grasp at $u = 0$) of the hand with two-phalanx fingers (a) and three-phalanx fingers (b). Pull directions of $\Psi = \pi/2$ (solid blue line), $\Psi = \pi/3$ (red dashed line), and $\Psi = \pi/6$ (black, dashed-dotted line) are shown, where Ψ is the angle between the palm surface and the displacement direction u. From the asterisk (*) onwards, there was no equilibrium of the fingers on the displaced object. (For interpretation of the references in colour in this figure legend, the reader is referred to the web version of this article.)

To interpret the performance results, we also calculated the work required to displace the object from its stable grasp equilibrium configuration. The resulting energy field is shown in the contour plots given in Fig. 7. Superimposed on these contour plots are the calculated displacement paths of the object pulled in the direction of $\pi/6$, $\pi/3$, and $\pi/2$ with respect to the palm. The construction lines perpendicular to the disturbance direction show that the object does indeed follow the path where these construction lines are tangent to the contour lines of the energy, which means that the object is in equilibrium in the direction perpendicular to the disturbance direction.

7. Discussion

In this discussion, we shall first address the way in which the calculated and measured results are interpreted before then going to consider the contribution made by our newly developed performance metrics in relation to the metrics available in the relevant literature.

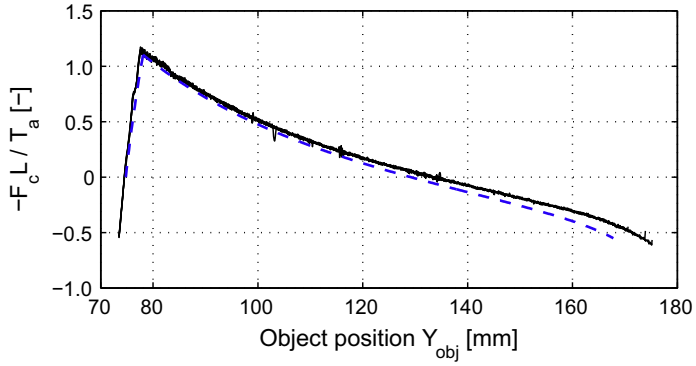

Fig. 6. Measured and calculated force–displacement characteristic of an object with a radius of $r_{obj} = 65$ mm grasped in the hand with two-phalanx fingers and pulled in a direction perpendicular to the palm ($\Psi = \pi/2$). The black solid lines show five repeated measurements starting from $Y_{obj} = 73.5$ mm and leading to the object position where all phalanges lost contact with the object. Along the blue dashed line the calculated characteristic starting from the calculated equilibrium position ($Y_{obj} = 74.8$ mm) and leading to the calculated position where all phalanges lose contact with the object ($Y_{obj} = 167.8$ mm) is shown. (For interpretation of the references in colour in this figure legend, the reader is referred to the web version of this article.)

7.1. The interpretation of the calculated and measured results

The ability to grasp cylindrical objects using fingers with two phalanges or three phalanges does differ slightly. In the case of both types of fingers, the lower limit is established when the finger tips collide against the palm. These smallest objects are grasped through contact with all the phalanges, while the object is simultaneously compressed against the palm. Objects that are larger than the upper limit can only be grasped by the distal phalanges. However, this pinching grasp is unstable and was therefore disregarded.

The maximum permitted disturbance force under which an object with a radius of $r_{obj} = 65$ mm can be held all depends on the disturbance direction. For both types of fingers, pulling the object in the $\pi/6$ direction in relation to the palm requires the least force out of all the calculated directions. Completely pulling the object out of the fingers that have two phalanges is easier than pulling it out of the fingers that have three phalanges. The direction that requires minimal force can be determined, but has not been elaborated in this paper.

The force–displacement characteristics (see Fig. 5) as well as the displacement trajectories (see Fig. 7) show discontinuities. At these points, the contact with one or more phalanges is lost. This can be visually represented by plotting the calculated contact forces and their resultant in one figure as was done in Fig. 8. At each peak of the force–displacement characteristic, one of the contact forces becomes zero. The object positions (X_{obj}, Y_{obj}) and finger configurations $\theta_{ij},\ p_{ij}$ where the contact with the phalanx *ij* is lost can be calculated by Eqs. (3)–(10), where for phalanx *ij* the geometric loop closure vector equation (3) as well as the zero contact force equation (9) holds. This was calculated for each phalanx of the two-phalanx and three-phalanx fingered hands that grasped the object that was $r_{obj} = 65$ mm. These positions are shown superimposed on the displacement trajectories Fig. 9. This figure shows that sharp edges in the displacement trajectories do indeed arise when a contact point is lost.

The combined plot for the measured and calculated force–displacement characteristic shows a high correlation, as was indeed already demonstrated in [48]. The calculations based on the static model developed in this paper seem accurate and satisfactory for predicting performance. Indeed, the ability to calculate performance in the design stage depends on the complexity of the models and on the proposed design. Modeling for instance spatial grasps, fingers with more phalanges or fingers with compliant mechanisms would require more calculation effort. However, for the *evaluation* of the performance of robotic or prosthetic hands, the benchmark tests are applicable for any hand. For every hand we can, of course, measure the size of the smallest and largest objects that can be grasped as well as the minimal force required to pull the object out of the hand.

The relevance of calculating the performance in the design stage not only relates to design optimization, but also to the observation and understanding of the behavior of underactuated hands. Based on the calculated work that is required to displace a grasped object like Fig. 7 and the force–displacement characteristics like Fig. 5, we could for instance prove that the grasp equilibrium achieved with just the distal phalanges is unstable (i.e. amounts to a saddle point in the energy function). This might explain the remarks reported in the literature to the effect that pinching grasps were hard to achieve (e.g. [16,27,4]). We were also able to explain the unexpected displacement trajectories with the sharp edges that were evidenced when pulling the object in various directions. In the near future, these energy functions and force–displacement characteristics will be further interpreted by the authors and implemented in the designing of new underactuated fingers.

7.2. Ability to grasp and hold in relation to the performance metrics given in the literature

Table 1 in Chapter 2 gave an overview of the existing performance metrics for the design and evaluation of underactuated hands. We observed that the performance metrics applied in the design stage are often not used in the evaluation stage and vice versa. Although metrics concerning the closing motion and the contact force characteristics can be necessary precondi-

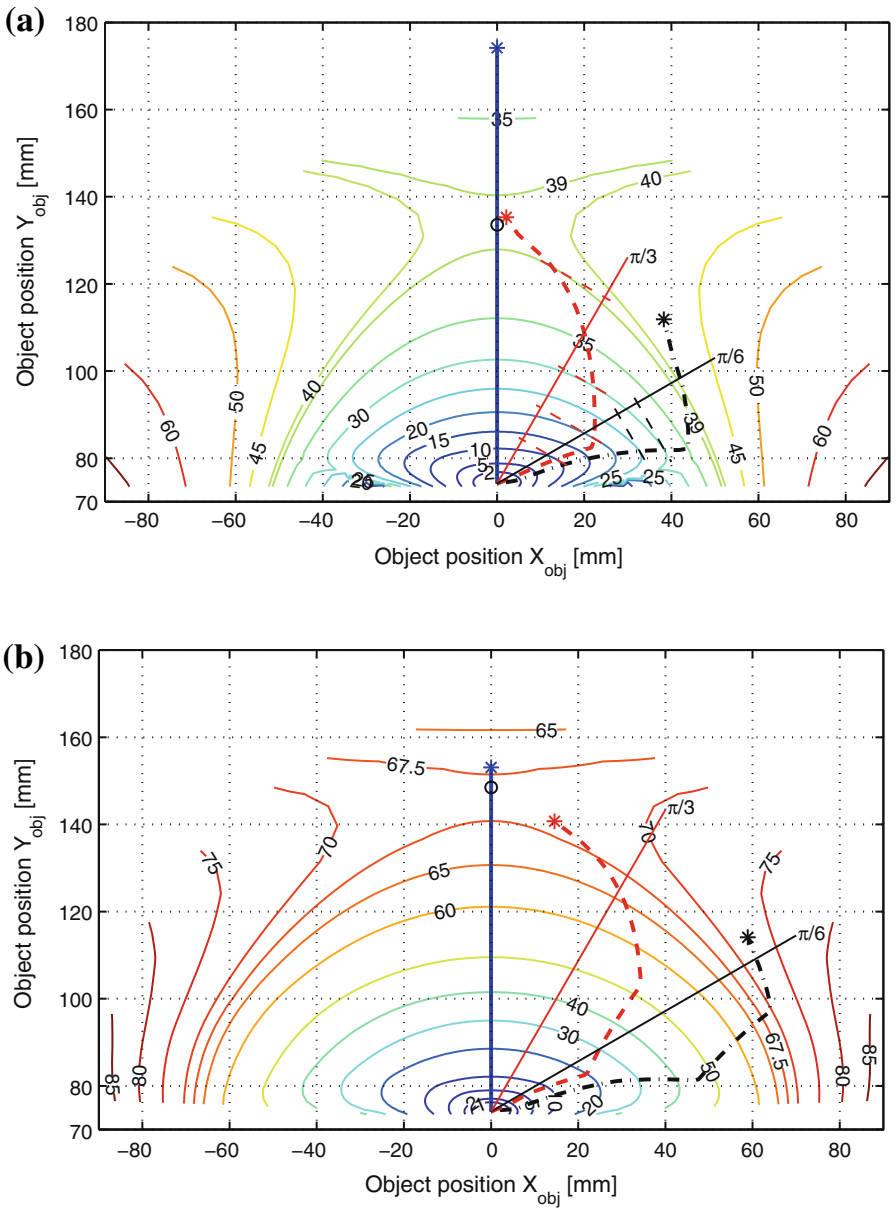

Fig. 7. Contour plots of the work required to displace the object with respect to the stable equilibrium position (energy minimum) for the hand with two-phalanx fingers (a) and three-phalanx fingers (b). An unstable equilibrium grasp (pinch grasp) is shown at the saddle point marked with 'o'. In both plots, the displacement trajectories of the object with a radius of $r_{obj} = 65$ mm and force disturbances in the direction of $\pi/2$ (blue, solid line), $\pi/3$ (red, dashed line), and $\pi/6$ (black, dashed dotted line) are given together with construction lines in these particular directions. The perpendicular dashed construction lines in (a) show that the disturbed object does indeed follow the trajectory tangent to the contour lines of the energy field. (For interpretation of the references in colour in this figure legend, the reader is referred to the web version of this article.)

tions, they are not sufficient to facilitate the grasping and holding of objects as required in, for instance, picking up and placing operations. In this section we shall discuss the contribution made by the newly developed benchmark tests with respect to the existing metrics given in the literature.

Most performance metrics found in the literature have been incorporated into the newly developed benchmark tests. For instance, the positiveness of the contact forces (1.2.1 in Table 1), their magnitude relative to the actuation force (1.2.3, 2.1.2) and, indirectly, their working direction (1.2.4, 2.1.3) are all incorporated in the quantification or calculation of the benchmark tests. In this paper, the intuitive evaluation of the ability to grasp as shown in pictures of various grasped objects (2.2.3), and the measurement of the forces required to pull objects out of the hand (2.3.2) are actually redefined to create a clear, uniform benchmark test that can be calculated as well as measured. Already in [30] a graph similar to the force–displacement curves obtained in this study was produced. However, it had still not been interpreted with respect to force disturbance rejection. Based on the calculated work required to displace grasped objects, we observed that in order to achieve a stable grasp without friction the objects do in fact have to be enveloped (2.2.1). Since moving an object from a stable grasp configuration always requires work, a form-closed grasp (2.3.1) can also be obtained when only the actuator movements are locked in such a stable grasp configuration.

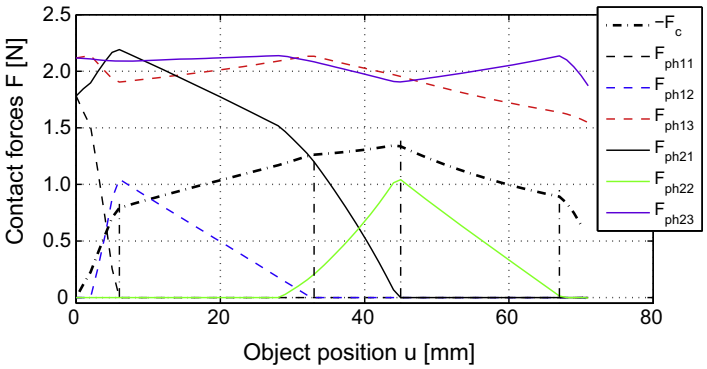

Fig. 8. Force–displacement characteristic (dashed-dotted line) for the object of $r_{obj} = 65$ mm grasped in the hand with three-phalanx fingers and disturbed in the $\pi/6$ direction together with the contact forces of all the phalanges as a function of the displacement u (mm). At the stable equilibrium point ($u = 0$), the middle phalanges are not in contact ($F_{ph_{i2}} = 0$). The magnitude of the contact forces and the number of phalanges in contact changed as a result of the reconfiguration of the fingers due to the displacement of the object. The vertical dashed lines show the sharp edges in the force–displacement characteristic where contact points with the phalanges are lost.

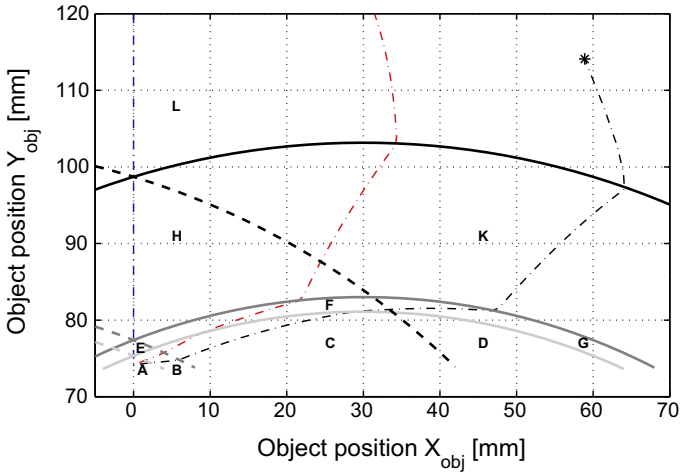

Fig. 9. Contact type transition lines relative to the object position (X_{obj}, Y_{obj}) for $r_{obj} = 65$ mm for the three-phalanx fingered hand together with the displacement trajectories for the object in the $\pi/2$ (blue), $\pi/3$ (red) and $\pi/6$ (black) directions. It shows that the sharp edges in the displacement trajectories arise during the transition from one contact type to the other. The left half plane is not shown here, but follows from the symmetry. The capital letters indicate the different contact type areas. With L and R denoting the left and right fingers, and the numbers to denote which phalanges are in contact, the contact types are as follows: A: L13-R13; B: L123-R13; C: L23-R13; D: L3-R13; E: L123-R123 (*power grasp*); F: L23-R123; G: L3-R123; H: L23-R23; K: L3-R23; L: L3-R3 (*pinch grasp*) where 1, 2, and 3 are the proximal, middle and distal phalanx, respectively. (For interpretation of the references in colour in this figure legend, the reader is referred to the web version of this article.)

Criteria which can be relevant, but which are not incorporated in the benchmark test are the considerations relating to the closing motion (1.1 in Table 1) and the constant magnitude of the resultant contact force relative to the actuation force (1.2.3, [2]). Fig. 8 shows that the performance metric regarding the constant isotropic distribution of the contact forces (1.2.2 and 2.1.1) conflicts with the benchmark tests. The distribution of the contact forces varies while the object is moving between the fingers, because such distribution very much depends on the position of the contact points of the phalanges. Therefore the assumption that there are fixed contact point positions in, for instance, the middle of all the phalanges is not true. Many grasp configurations may exist where one or more phalanges have no contact at all.

The main contribution made by the new performance metrics developed in this paper lies in the combination and extension of the existing metrics which will ultimately augment benchmark tests. These tests can be applied to calculations (i.e. in the design stage) as well as to measurements (i.e. at the evaluation stage) concerning the ability to grasp and the ability to hold various objects in underactuated hands. These benchmark tests are closely related to functional requirements on picking up and placing operations like the range of object sizes which can be grasped and the maximum permitted accelerations of the grasped object.

8. Conclusion

The objectives of this paper were to determine the performance metrics that address the ability of underactuated hands to pick up and place various objects, and to furthermore assess these new metrics through simulations as well as through

experiments. On the basis of a literature review, we conclude that there is a big difference between metrics applied in the design stage and metrics applied in the evaluation stage. In addition, there was in fact no previous benchmark test that could be said to be directly related to the capability of underactuated hands to pick up and place various objects.

The *ability to grasp* is a new performance metric that quantifies the ability to achieve stable equilibrium in a range of freely moving, cylindrical objects just by using the fingers and the palm of the hand. The capability to keep the grasped objects within the hand while disturbing forces are applied to the objects in question can be quantified by the *ability to hold*. These new performance metrics constitute a combination and extension of existing metrics.

The new performance metrics can be calculated by using a static grasp model of the type developed in this study and reported in this paper. This model is applicable to any conventional underactuated hand. This model takes into account the fact that underactuated fingers passively reconfigure to obtain grasp equilibrium and to resist disturbing forces. The application of this model to a cable-pulley driven hand with two fingers and either two or three phalanges demonstrated that the latter performs slightly better than the first. Preliminary experiments demonstrated the accuracy of the predicted performance.

With the grasp model, the work required to displace objects within the hand can also be calculated. The resulting energy field can be used to determine the stability of the grasp equilibrium configurations, the displacement trajectories of an object while subjected to force disturbances, the minimum work required to completely pull the object out of the hand, and, finally, the stability area in which a grasped object is attracted to a stable grasp configuration by the fingers of the underactuated hand.

Acknowledgments

This work was carried out as part of the FALCON project under responsibility of the Embedded System Institute with Vanderlande Industries as the industrial partner. This project is partially supported by the Dutch Ministry of Economic Affairs within the framework of the Embedded System Institute (BSIK03021) program.

References

[1] I. Kato, K. Sadamoto, Mechanical Hands Illustrated, Hemisphere Publishing Corporation, 1987.
[2] H. de Visser, J.L. Herder, Force-directed design of a voluntary closing hand prosthesis, Journal of Rehabilitation Research and Development 37 (2000) 261–271.
[3] Y. Kamikawa, T. Maeno, Underactuated five-finger prosthetic hand inspired by grasping force distribution of humans, in: Proceedings of the IEEE/RSJ International Conference on Intelligent Robots and Systems (IROS), 2008, pp. 717–722.
[4] T. Laliberté, L. Birglen, C.M. Gosselin, Underactuation in robotic grasping hands, Machine Intelligence and Robotic Control 4 (3) (2002) 1–11.
[5] V. Bégoc, S. Krut, E. Dombre, C. Durand, F. Pierrot, Mechanical design of a new pneumatically driven underactuated hand, in: Proceedings of the IEEE International Conference on Robotics and Automation (ICRA), 2007, pp. 927–933.
[6] L. Birglen, T. Laliberté, C.M. Gosselin, in: B. Siciliano, O. Khatib, F. Groen (Eds.), Underactuated Robotic Hands, Springer Tracts in Advanced Robotics, vol. 40, Springer-Verlag, Berlin, Heidelberg, 2008.
[7] V. Bégoc, C. Durand, S. Krut, E. Dombre, F. Pierrot, On the form-closure capability of robotic underactuated hands, in: Proceedings of the International Conference on Control, Automation, Robotics, and Vision, 2006, pp. 1–8.
[8] G.A. Kragten, J.L. Herder, Equilibrium, stability, and robustness in underactuated grasping, in: Proceedings of the ASME International Design Engineering Technical Conferences (IDETC), MECH34963, 2007.
[9] European Robotics Research Network (EURON), Benchmarking initiative: manipulation and grasping. <http://www.euron.org/activities/benchmarks/grasping> (retrieved 26.01.09).
[10] A. Bicchi, Hands for dexterous manipulation and robust grasping: a difficult road toward simplicity, IEEE Transactions on Robotics and Automation 16 (6) (2000) 652–662.
[11] L. Zollo, S. Roccella, E. Guglielmelli, M. Carrozza, P. Dario, Biomechatronic design and control of an anthropomorphic artificial hand for prosthetic and robotic applications, IEEE/ASME Transactions on Mechatronics 12 (4) (2007) 418–429.
[12] B. Massa, S. Roccella, M.C. Carrozza, P. Dario, Design and development of an underactuated prosthetic hand, in: Proceedings of the IEEE International Conference on Robotics and Automation (ICRA), vol. 4(4), 2002, pp. 3374–3379.
[13] L. Wu, G. Carbone, M. Ceccarelli, Designing an underactuated mechanism for a 1 DOF finger operation, Mechanism and Machine Theory 44 (2) (2009) 336–348.
[14] J.D. Crisman, C. Kanojia, I. Zeid, Graspar: a flexible easily controllable robotic hand, IEEE Robotics and Automation Magazine 3 (2) (1996) 32–38.
[15] S. Schulz, C. Pylatiuk, G. Bretthauer, A new ultralight anthropomorphic hand, in: Proceedings of the IEEE International Conference on Robotics and Automation (ICRA), vol. 3, 2001, pp. 2437–2441.
[16] M.C. Carrozza, G. Cappiello, S. Micera, B.B. Edin, L. Beccai, C. Cipriani, Design of a cybernetic hand for perception and action, Biological Cybernetics 95 (2006) 629–644.
[17] S. Hirose, Y. Umetani, The development of soft gripper for the versatile robot hand, Mechanism and Machine Theory 13 (3) (1978) 351–359.
[18] S. Krut, A force-isotropic underactuated finger, in: Proceedings of the IEEE International Conference on Robotics and Automation (ICRA), 2005, pp. 2314–2319.
[19] K. Fite, T. Withrow, X. Shen, K. Wait, J. Mitchell, M. Goldfarb, A gas-actuated anthropomorphic prosthesis for transhumeral amputees, IEEE Transactions on Robotics 24 (1) (2008) 159–169.
[20] W. Townsend, The BarrettHand grasper – programmably flexible part handling and assembly, Industrial Robot: An International Journal 27 (3) (2000) 181–188.
[21] M.C. Carrozza, C. Suppo, F. Sebastiani, B. Massa, F. Vecchi, R. Lazzarini, M.R. Cutkosky, P. Dario, The SPRING hand: development of a self-adaptive prosthesis for restoring natural grasping, Autonomous Robots 16 (2) (2004) 125–141.
[22] J.-U. Chu, D.-H. Jung, Y.-J. Lee, Design and control of a multifunction myoelectric hand with new adaptive grasping and self-locking mechanisms, in: Proceedings of the IEEE International Conference on Robotics and Automation (ICRA), 2008, pp. 743–748.
[23] W. Zhang, Q. Chen, Z. Sun, D. Zhao, Under-actuated passive adaptive grasp humanoid robot hand with control of grasping force, in: Proceedings of the IEEE International Conference on Robotics and Automation (ICRA), vol. 1, 2003, pp. 696–701.
[24] W. Zhang, Q. Chen, Z. Sun, L. Xu, Superunderactuated multifingered hand for humanoid robot, Frontiers of Mechanical Engineering in China 1 (2006) 33–39.

[25] R. Cabás, L. Cabás, C. Balaguer, Optimized design of the underactuated robotic hand, in: Proceedings of the IEEE International Conference on Robotics and Automation (ICRA), 2006, pp. 982–987.
[26] E. Boudreault, C.M. Gosselin, Design of sub-centimetre underactuated compliant grippers, in: Proceedings of the ASME International Design Engineering Technical Conferences (IDETC), MECH99415, 2006.
[27] C.M. Gosselin, F. Pelletier, T. Laliberté, An anthropomorphic underactuated robotic hand with 15 dofs and a single actuator, in: Proceedings of the IEEE International Conference on Robotics and Automation (ICRA), 2008, pp. 749–754.
[28] A.M. Dollar, R.D. Howe, Towards grasping in unstructured environments: grasper compliance and configuration optimization, Advanced Robotics 19 (5) (2005) 523–543.
[29] M. Myrand, C.M. Gosselin, Dynamic simulation of an underactuated hand for space applications, in: CISM-IFToMM Symposium on Robot Design, Dynamics, and Control (RoManSy), 2004.
[30] T. Laliberté, C.M. Gosselin, Simulation and design of underactuated mechanical hands, Mechanism and Machine Theory 33 (1/2) (1998) 39–57.
[31] J. Schuurmans, R.Q. van der Linde, D.H. Plettenburg, F.C.T. van der Helm, Grasp force optimization in the design of an underactuated robotic hand, in: Proceedings of the IEEE International Conference on Rehabilitation Robotics (ICORR), 2007, pp. 776–782.
[32] L.M. Sie, C.M. Gosselin, Dynamic simulation and optimization of underactuated robotic fingers, in: Proceedings of the ASME International Design Engineering Technical Conferences (IDETC), MECH34220, 2002.
[33] A.M. Dollar, R.D. Howe, The SDM hand as a prosthetic terminal device: a feasibility study, in: Proceedings of the IEEE International Conference on Rehabilitation Robotics (ICORR), 2007, pp. 978–983.
[34] G. Figliolini, P. Rea, Ca.U.M.Ha. robotic hand (Cassino-Underactuated-Multifinger-Hand), in: Proceedings of the IEEE/ASME International Conference on Advanced Intelligent Mechatronics, 2007, pp. 1–6.
[35] C. Cipriani, F. Zaccone, G. Stellin, L. Beccai, G. Cappiello, M. Carrozza, P. Dario, Closed-loop controller for a bio-inspired multi-fingered underactuated prosthesis, in: Proceedings of the IEEE International Conference on Robotics and Automation (ICRA), 2006, pp. 2111–2116.
[36] J.P. Jobin, H.S. Buddenberg, J.L. Herder, An underactuated prosthesis finger mechanism with rolling joints, in: Proceedings of the ASME International Design Engineering Technical Conferences (IDETC), MECH57192, 2004.
[37] R. Rizk, S. Krut, E. Dombre, Grasp-stability analysis of a two-phalanx isotropic underactuated finger, in: Proceedings of the IEEE/RSJ International Conference on Intelligent Robots and Systems (IROS), 2007, pp. 3289–3294.
[38] R. Doshi, C. Yeh, M. LeBlanc, The design and development of a gloveless endoskeletal prosthetic hand, Journal of Rehabilitation Research and Development 35 (4) (1998) 388–395.
[39] H. Huang, L. Jiang, Y. Liu, L. Hou, H. Cai, H. Liu, The mechanical design and experiments of HIT/DLR prosthetic hand, in: Proceedings of the IEEE International Conference on Robotics and Biomimetics (ROBIO), 2006, pp. 896–901.
[40] L. Birglen, C.M. Gosselin, Optimal design of 2-phalanx underactuated fingers, in: Conference on Intelligent Manipulation and Grasping, 2004.
[41] M. Carrozza, F. Vecchi, F. Sebastiani, G. Cappiello, S. Roccella, M. Zecca, R. Lazzarini, P. Dario, Experimental analysis of an innovative prosthetic hand with proprioceptive sensors, in: Proceedings of the IEEE International Conference on Robotics and Automation (ICRA), vol. 2, 2003, pp. 2230–2235.
[42] M. Carrozza, G. Cappiello, G. Stellin, F. Zaccone, F. Vecchi, S. Micera, P. Dario, A cosmetic prosthetic hand with tendon driven under-actuated mechanism and compliant joints: ongoing research and preliminary results, in: Proceedings of the IEEE International Conference on Robotics and Automation (ICRA), 2005, pp. 2661–2666.
[43] R.M. Crowder, V.N. Dubey, P.H. Chappell, D.R. Whatley, A multi-fingered end effector for unstructured environments, in: Proceedings of the IEEE International Conference on Robotics and Automation (ICRA), vol. 4, 1999, pp. 3038–3043.
[44] V.N. Dubey, R.M. Crowder, Evolution of a novel finger mechanism for robust industrial end effectors, in: Proceedings of the ASME International Design Engineering Technical Conferences (IDETC), MECH49999, 2008.
[45] N. Fukaya, S. Toyama, T. Asfour, R. Dillmann, Design of the TUAT/Karlsruhe humanoid hand, in: Proceedings of the IEEE/RSJ International Conference on Intelligent Robots and Systems (IROS), 2000, pp. 1754–1759.
[46] A. van Lunteren, G.H.M. van Lunteren-Gerritsen, On the use of prostheses by children with a unilateral congenital forearm defect, Journal of Rehabilitation Sciences 2 (1) (1989) 10–12.
[47] G.A. Kragten, A.C. Kool, J.L. Herder, Ability to hold grasped objects by underactuated hands: performance prediction and experiments, in: Proceedings of the IEEE International Conference on Robotics and Automation (ICRA), 2009, 2493–2498.
[48] G.A. Kragten, J.L. Herder, A platform for grasp performance assessment in compliant or underactuated hands, Journal of Mechanical Design, 2009, accepted for publication.